AFRL-RX-WP-TP-2010-4147

PROBABILISTIC SENSITIVITY ANALYSIS WITH RESPECT TO BOUNDS OF TRUNCATED DISTRIBUTIONS (PREPRINT)

H. Millwater and Y. Feng

University of Texas at San Antonio

APRIL 2010

AIR FORCE RESEARCH LABORATORY
MATERIALS AND MANUFACTURING DIRECTORATE
WRIGHT-PATTERSON AIR FORCE BASE, OH 45433-7750
AIR FORCE MATERIEL COMMAND
UNITED STATES AIR FORCE

REPORT DOCUMENTATION PAGE

Form Approved
OMB No. 0704-0188

1. REPORT DATE *(DD-MM-YY)*	2. REPORT TYPE	3. DATES COVERED *(From - To)*
April 2010	Journal Article Preprint	01 April 2010 – 01 April 2010

4. TITLE AND SUBTITLE
PROBABILISTIC SENSITIVITY ANALYSIS WITH RESPECT TO BOUNDS OF TRUNCATED DISTRIBUTIONS (PREPRINT)

5a. CONTRACT NUMBER
In-house

5b. GRANT NUMBER

5c. PROGRAM ELEMENT NUMBER
62102F

6. AUTHOR(S)
H. Millwater and Y. Feng

5d. PROJECT NUMBER
4347

5e. TASK NUMBER
RG

5f. WORK UNIT NUMBER
M02R3000

7. PERFORMING ORGANIZATION NAME(S) AND ADDRESS(ES)
University of Texas at San Antonio
San Antonio, TX 78249

8. PERFORMING ORGANIZATION REPORT NUMBER
AFRL-RX-WP-TP-2010-4147

9. SPONSORING/MONITORING AGENCY NAME(S) AND ADDRESS(ES)
Air Force Research Laboratory
Materials and Manufacturing Directorate
Wright-Patterson Air Force Base, OH 45433-7750
Air Force Materiel Command
United States Air Force

10. SPONSORING/MONITORING AGENCY ACRONYM(S)
AFRL/RXLMN

11. SPONSORING/MONITORING AGENCY REPORT NUMBER(S)
AFRL-RX-WP-TP-2010-4147

12. DISTRIBUTION/AVAILABILITY STATEMENT
Approved for public release; distribution unlimited.

13. SUPPLEMENTARY NOTES
Journal article submitted to *AIAA Journal*. PAO Case Number: 88ABW-2010-1275; Clearance Date: 17 Mar 2010.

This work was funded in whole or in part by Department of the Air Force. The U.S. Government has for itself and others acting on its behalf an unlimited, paid-up, nonexclusive, irrevocable worldwide license to use, modify, reproduce, release, perform, display, or disclose the work by or on behalf of the U.S. Government. Paper contains color.

14. ABSTRACT

Bounds on variables are often implemented as part of a quality control program to ensure a sufficient pedigree of a product component and these bounds may significantly affect the product's design through constraints such as cost, manufacturability and reliability. Thus, it is useful to determine the sensitivity of the product reliability to the imposed bounds. In this work, a method to compute the partial derivatives of the probability-of-failure and the response moments, such as mean and the standard deviation, with respect to the bounds of truncated distributions are derived for rectangular truncation. The sensitivities with respect to the bounds are computed using a supplemental "flux" integral that can be combined with the probability-of-failure or response moment information. The formulation is exact in the sense that the accuracy depends only upon the numerical algorithms employed. The flux integral is formulated as a special case of the probability integral for which the sensitivities are being computed.

15. SUBJECT TERMS
constraints, probability-of-failure, response moments

16. SECURITY CLASSIFICATION OF:			17. LIMITATION OF ABSTRACT:	18. NUMBER OF PAGES	19a. NAME OF RESPONSIBLE PERSON (Monitor)
a. REPORT	b. ABSTRACT	c. THIS PAGE			Reji John
Unclassified	Unclassified	Unclassified	SAR	60	19b. TELEPHONE NUMBER *(Include Area Code)* N/A

Standard Form 298 (Rev. 8-98)
Prescribed by ANSI Std. Z39-18

Probabilistic Sensitivity Analysis with respect to Bounds of Truncated Distributions

H. Millwater and Y. Feng

Department of Mechanical Engineering

University of Texas at San Antonio

Abstract

Bounds on variables are often implemented as part of a quality control program to ensure a sufficient pedigree of a product component and these bounds may significantly affect the product's design through constraints such as cost, manufacturability and reliability. Thus, it is useful to determine the sensitivity of the product reliability to the imposed bounds. In this work, a method to compute the partial derivatives of the probability-of-failure and the response moments, such as mean and the standard deviation, with respect to the bounds of truncated distributions are derived for rectangular truncation. The sensitivities with respect to the bounds are computed using a supplemental "flux" integral that can be combined with the probability-of-failure or response moment information. The formulation is exact in the sense that the accuracy depends only upon the numerical algorithms employed. The flux integral is formulated as a special case of the probability integral for which the sensitivities are being computed. As a result, the methodology can be implemented with any probabilistic method, such as sampling, first order reliability method, conditional expectation, etc. Moreover, the maximum and minimum values of the sensitivities can be obtained without any additional computational cost. The methodology is quite general and can be applied to both

component and system reliability. Several numerical examples are presented to demonstrate the advantages of the proposed method. In comparison, the examples using Monte Carlo sampling demonstrated that the flux-based methodology achieved the same accuracy as a standard finite difference approach using approximately 4 orders of magnitude fewer samples. This is largely due to the fact that this method does not rely upon subtraction of two near-equal numbers.

Notation

a	lower boundary of truncated distribution
b	upper boundary of truncated distribution
E	expected value operator
$f_X(a)$	marginal PDF of truncated distribution evaluated at lower boundary a
$f_X(b)$	marginal PDF of truncated distribution evaluated at upper boundary b
$f_{\mathbf{X}}(\mathbf{x})$	joint probability density function (JPDF)
g	limit state
$I(\mathbf{x})$	indicator function ($I(\mathbf{x}) = 1$ in failure region, and 0 otherwise)
JPDF	joint probability density function represented by $f_{\mathbf{X}}(\mathbf{x})$
N	number of random variables
P_f	probability-of-failure
P_I^{θ}	flux integral of probability-of-failure at bound θ
$\mathbf{X}$	vector of random variables, $\mathbf{X} = (X_1,\ldots,X_N)$
$\mathbf{Y}$	vector of random variables $\mathbf{X}$ excluding X_i, $\mathbf{Y} = (X_1,\ldots,X_{i-1},X_{i+1},\ldots,X_N)$

Z response function of random variables

Γ_I flux of JPDF in failure domain across the truncation boundary

Γ_Z flux of response times the JPDF across the truncation boundary

Γ_{Z^2} flux of response squared times the JPDF across the truncation boundary

κ_a kernel function with respect to lower bound

κ_b kernel function with respect to upper bound

μ_Z mean of response function Z

σ_Z standard deviation of response function Z

θ lower or upper bound of PDF

1. Introduction

In any design problem it is important to define approved allowables for material properties, joint properties, fracture properties, dimensioning tolerances, etc. Oftentimes allowables arise from and are implemented within a quality assurance (QA) program which may establish bounds on allowables and ensure that values outside of the allowables will not be accepted in order to guarantee the quality of a product. For example, cases in point include “A” (99% probability, 95% confidence) and “B” (90% probability, 95% confidence) basis allowables. That is, for an “A” basis allowable, there is a 95 percent probability that 99 percent of the samples will be less than or greater than (depending on the application) the numerical allowable. For a “B” basis allowable, there is a 95 percent probability that 90 percent of the samples will be less than or greater than the numerical allowable.

Another common occurrence arises with respect to geometric random variables obtained by machining. Tolerance limits (plus and minus) are placed upon dimensions that are the result of machining operations, e.g., holes, fillet radii, and seal diameters. Correct dimensioning in the part is necessary for subsequent assembly and to minimize stress concentrations. The QA operations ensure that dimensions outside of the tolerances will not be present in the finished product.

For these cases, it is easy to see that the implementation of a QA program will often result in truncated distributions that affect the overall quantity or cost of a product. If material properties are outside of the allowables or dimensions outside of tolerances are removed before production, then effectively, the quantity can be modeled as a truncated distribution. Typical cases include truncated normal, Weibull and uniform distributions.

Truncated distributions can also arise naturally when modeling nonparametric distributions. For example, loading variability is often modeled nonparametrically through an exceedance curve that defines the number of occurrences of loads (often accelerations or g-forces) that exceed different load levels [1, 2]. The upper limit to the exceedance curve is presumed, but often not verified, to be sufficiently large such that further data collection will not affect the design of the structure. A similar condition arises with respect to defects in gas turbine materials where a nonparametric distribution is used to model the probability of defect size [3]. This distribution is then used as part of the process to certify that the design is within allowable limits on the probability-of-failure. A truncated distribution in the context of this research encompasses any distribution that has non-zero PDF value at either bound of its domain.

Establishment of the allowables for material qualification for a new material or a new application of the material is typically based on extensive testing and is often costly in terms of schedule and funds. Therefore, it is useful to have some tools to assess, in the design stage, the impact the bounds have on the product reliability, cost, manufacturability, etc. Therefore, methods to compute the sensitivity of the reliability (or probability-of-failure) of a component or system with respect to the bounds of truncated random variables would be a useful tool to assist in setting appropriate values for the bounds and to assess the performance of the design.

The finite difference method can be used to estimate the numerical derivative of the probability-of-failure with respect to a random variable bound, e.g. perturb a bound, rerun the analysis and compute the ratio of the differences $\frac{\partial P_f}{\partial \theta_i} \approx \frac{P(\theta + \Delta\theta) - P(\theta)}{\Delta\theta}$. This approach is error prone, however, as the amount of the perturbation, $\Delta\theta$, can strongly affect the accuracy of the calculation and the numerical estimate usually suffers from subtraction error. Moreover, a small perturbation is needed to obtain an accurate derivative. As a result, the derivative estimate requires a subtraction of two probabilities that differ only slightly. If sampling is used to obtain the probability, a very large number of samples may be required to reduce sampling variance before the subtraction operation. These issues make finite differencing error prone and arduous before obtaining confidence in the result.

There are a number of probabilistic sensitivity methods that provide valuable information during the design process, often with little additional computational cost. Frey and S.R. Patil provide an overview article discussing ten sensitivity methods, both probabilistic and deterministic [4]. Helton et al. discusses the use of scatter plots,

regression analysis, and Spearman or Pearson correlation and other methods as qualitative and quantitative metrics for sampling methods as inexpensive approaches to discerning the contribution of the variance of each random variable to the output [5].

Variance-based methods based [6, 7] are capable of apportioning the amount of variance in the output variance to the variance of the inputs, thus, providing a method to rank order the key inputs. The method is applicable to monotonic and nonmonotonic models. Calculation of the sensitivity indices requires computation in addition to the probability-of-failure calculation by requiring multiple multidimensional integrals. The Fourier Amplitude Sensitivity Test (FAST) method can be used to reduce the multidimensional integrals into a one-dimensional integral [8]. Lui et al. use the Kullback-Leibler relative entropy-based method to evaluate the impact of a random variable on a design performance by measuring the divergence between two probability density functions of the performance response, obtained before and after the variation reduction of the random variable [9]. The application is similar to the variance-based methods but is not limited to differences in the second moment.

A number of sensitivity methods are available for the First Order Reliability Method (FORM). Sensitivity factors (derivatives of the safety index with respect to the random variables) [10], derivatives of the probability of failure with respect to the random variable parameters, e.g., $\partial P/\partial \mu$, $\partial P/\partial \sigma$ [10] and omission factors [11] are computed as by-products of an analysis. Each of these indexes provides an indication as to the importance of the parameters.

Various authors develop and discuss the “Score Function” method for the computation of partial derivatives of a performance function (probability-of-failure or

response moment) with respect to parameters of the underlying input probability distributions [12-17]. This method provides local partial derivatives of the probability-of-failure or response moments with respect to the parameters of the input PDFs, e.g., $\partial P/\partial \mu,\ \partial P/\partial \sigma$. Implementation of the methodology is convenient using sampling methods. A significant advantage is that negligible additional computing time is required to determine the sensitivities.

None of aforementioned methods explicitly treat the sensitivity of the probability-of-failure or the response moments with respect to the bounds of a distribution. Therefore, a new methodology is derived and demonstrated below. The mathematical formulation follows the development of the Score Function method [13]. However, as shown below, an additional flux integral is required that is not present in the traditional Score Function formulation. This flux integral is also a probability integral. On the other hand, other aspects of this formulation simplify relative to the traditional Score Function approach. The implications are that the resulting equations can be solved with any probabilistic method such as sampling, the First Order Reliability Method, conditional expectation, importance sampling, and others.

The rest of this paper is organized as follows. The basic formulation of the governing equations for sensitivities of the probability-of-failure is presented in Section 2. Section 3 describes the extension of the method to compute sensitivities with respect to response moments. Section 4 provides numerical examples and Section 5 contains discussion and conclusions.

2. Basic Formulation

2.1 Governing Equations

The methodology developed here can be considered as an extension of the Score Function method [13]. Given a joint probability density function (JPDF) $f_{\mathbf{x}}(\mathbf{x})$, the probability-of-failure can be defined as

$$P_f = \int_{g(\mathbf{x})\le 0} f_x(\mathbf{x}) d\mathbf{x} \qquad \textbf{(1)}$$

where $\mathbf{X}$ is a vector of random variables of length N, $\mathbf{X} = (X_1,\ldots,X_N)$, g is the limit state function where $g(\mathbf{x}) \le 0$ defines the failure domain, and the integral is N dimensional.

In this paper, the focus is on developing sensitivities with respect to bounds of truncated distributions, that is, probability distributions whose range is finite in at least one direction and whose PDF value at the finite range is nonzero. In addition, only rectangular truncation is considered, i.e., $x_i = \theta_i : \theta_i \in \mathbf{R}^n$ where θ_i corresponds to the lower or upper bound of the distribution f_{X_i}. Sensitivities with respect to means and standard deviations of truncated distributions have been discussed previously [18]. Related developments on sensitivities with respect to PDF parameters for nontruncated distributions can be found in [13,18]

Introducing the indicator function $I(\mathbf{x})$, which is defined as equal to one if $g(\mathbf{x}) \le 0$ and zero otherwise, the probability-of-failure integral can be written

$$P_f = \int_{-\infty}^{\infty} I(\mathbf{x}) f_{\mathbf{X}}(\mathbf{x}) d\mathbf{x} \qquad \textbf{(2)}$$

The derivative of the probability integral with respect to a parameter of a random variable that affects the boundary can be determined by using the idea of the classical Reynold's Transport Theorem:

$$\frac{D}{Dt}\int_V \Psi(\mathbf{x},t)dV = \int_V \frac{\partial \Psi(\mathbf{x},t)}{\partial t}dV + \int_S \Psi(\mathbf{x},t)v_j n_j dS \qquad \textbf{(3)}$$

where Ψ is a property of the continuum, v denotes the velocity of the material, $\boldsymbol{n}$ represents the unit normal along the boundary S, and V is the volume enclosed by S. The surface integral term in Eq. (3) is the value of Ψ on the boundary multiplied by the volume swept by the particles on the boundary in the time interval dt, integrated over dS. This term can be considered as a flux of the property Ψ over the surface S. The total derivative, D/Dt, is also known as the material derivative [19].

The concept of the material derivative can be utilized to take the derivative of the probability integral, Eq. (2), with respect to a bound of a random variable PDF. Here, the independent parameter, θ_i, is a bound of the distribution representing X_i, the JPDF is equivalent to the property Ψ, the volume is the N dimensional random variable space, and *S* is the surface of the random variable space remaining when random variable X_i is set to the bound θ_i. For rectangular truncation, the surface *S* is straightforward to compute as the independent parameter, θ_i, is a bound of the N dimensional random variable space.

The unit normal and the equivalent velocity term and their relation can be discerned from a problem of two random variables, see Figure 1. Since the independent parameter θ is an element of *X*, the velocity becomes $v = \partial x/\partial\theta = 1$. At the lower bound

ν and $\boldsymbol{n}$ are in opposite directions, hence, the dot product $\nu_j n_j$ equals -1. At the upper bound $\nu_j n_j$ equals +1.

Applying these concepts to the probability-of-failure integral yields the equation

$$\frac{\partial P_f}{\partial \theta_i} = \int_{-\infty}^{\infty} I(\mathbf{x},\theta_i) \frac{\partial f_{\mathbf{X}}(\mathbf{x},\theta_i)}{\partial \theta_i} d\mathbf{x} \pm \int_{-\infty}^{\infty} I(\mathbf{y},\theta_i) f_{\mathbf{X}}(\mathbf{y},\theta_i) d\mathbf{y} \quad \textbf{(4)}$$

where $\mathbf{Y}$ denotes the vector of the random variables $\mathbf{X}$ but excluding X_i, i.e., $\mathbf{Y} = (X_1,\ldots,X_{i-1},X_{i+1},\ldots,X_N)$, $f_{\mathbf{X}}(\mathbf{y},\theta_i)$ represents the conditional JPDF given $x_i = \theta_i$, and the "+" sign is used when θ_i represents the upper bound and "-" for the lower bound.

Using the concept of kernel functions [18] defined as $\kappa_{\theta_i}(\mathbf{x}) = \frac{\partial f_{\mathbf{X}}(\mathbf{x})}{\partial \theta_i} \frac{1}{f_{\mathbf{X}}(\mathbf{x})}$, Eq. (4) can be written

$$\frac{\partial P_f}{\partial \theta_i} = \int_{-\infty}^{\infty} I(\mathbf{x}) \kappa_\theta(\mathbf{x}) f_{\mathbf{X}}(\mathbf{x}) d\mathbf{x} \pm \int_{-\infty}^{\infty} I(\mathbf{y},\theta_i) f_{\mathbf{X}}(\mathbf{y},\theta_i) d\mathbf{y} \quad \textbf{(5)}$$

The kernel functions with respect to a bound for a truncation value of random variable X_i are (see appendix A)

$$\kappa_a = \frac{\partial f_{\mathbf{X}}(\mathbf{x})}{\partial a} \frac{1}{f_{\mathbf{X}}(\mathbf{x})} = f_{X_i}(a) \quad \textbf{(6)}$$

$$\kappa_b = \frac{\partial f_{\mathbf{X}}(\mathbf{x})}{\partial b} \frac{1}{f_{\mathbf{X}}(\mathbf{x})} = -f_{X_i}(b) \quad \textbf{(7)}$$

where a and b represent the lower and upper bound, respectively, of X_i. It is quite remarkable that the magnitude of the kernel functions are independent of $\mathbf{X}$, equal to the value of the marginal PDF of X_i evaluated at the respective bound, and independent of the form of the JPDF. In a subsequent section, we demonstrate that the kernel functions

must have these mathematical forms in order to satisfy the requirement that the derivative of the probability-of-failure equals zero for the case where the indicator function is everywhere one.

The flux surface integral $\Gamma_I^\theta = \int_{-\infty}^{\infty} I(\mathbf{y},\theta) f_{\mathbf{X}}(\mathbf{y},\theta) d\mathbf{y}$ can be rewritten since the JPDF can be simplified as $f_{\mathbf{X}}(\mathbf{y},\theta) = f_{X_i}(\theta) f_{\mathbf{Y}}(\mathbf{y})$ yielding

$$\Gamma_I^\theta = f_{X_i}(\theta) \int_{-\infty}^{\infty} I(\mathbf{y},\theta) f_{\mathbf{Y}}(\mathbf{y}) d\mathbf{y} = f_{X_i}(\theta) P_I^\theta \quad \textbf{(8)}$$

where $P_I^\theta = \int_{-\infty}^{\infty} I(\mathbf{y},\theta) f_{\mathbf{Y}}(\mathbf{y}) d\mathbf{y}$ and the subscript I denotes the dependence on the indicator function. Since P_I^θ is a probability integral, it is always positive. Using the kernel functions from Eqs. (6) and (7), the surface integral, Eq. (8), the fact that $P_f = E[I(\mathbf{x})]$, and the proper sign for each bound, the equations for the sensitivities become

$$\frac{\partial P_f}{\partial a_i} = f_{X_i}(a)(P_f - P_I^a) \quad \textbf{(9)}$$

$$\frac{\partial P_f}{\partial b_i} = -f_{X_i}(b)(P_f - P_I^b) \quad \textbf{(10)}$$

Thus, the effort to obtain the sensitivities becomes one of evaluating the flux integrals P_I^a and P_I^b in addition to the probability-of-failure.

2.2 Evaluation of flux integral

The flux integral can be evaluated by integrating the JPDF times the indicator function over the surface *S* defined by the condition $x_i = \theta$. That is, one integrates the JPDF in the failure region over the surface S. Thus, the dimension of the flux integral is

N-1. A schematic of the flux in two dimensions (two random variable problem) is shown in Figure 2 where the value of the joint PDF along the upper bound of X_1 is outlined. Mathematically, the flux is computed as

$$\Gamma_I^\theta = f_{X_i}(\theta) P_I^\theta \tag{11}$$

For problems with one random variable, the flux reduces to $f_{\mathrm{X}}(a)$ over the lower bound and $f_{\mathrm{X}}(b)$ over the upper bound and Eqs. (9) and (10) reduce to the well-known Leibnitz rule in one dimension.

Figure 3 shows the failure domain for several problems of two random variables. In each case, the failure domain fully encompasses the upper bound of random variable X_1 and does not encompass any of the lower bound. Therefore, given the same JPDF, each problem has the same flux integral with respect to the bounds, that is, the flux integral depends only upon the failure definition along the boundary *S* and not by the definition of failure throughout the failure domain. For the examples given in Figure 3, $P_I^a = 0$ and $P_I^b = 1$.

Evaluation of Eq. (11) requires an N-1 dimensional integral. However, the flux integral is also a probability integral, which can be considered as a special case of the probability-of-failure integral, Eq. (2). Therefore, the flux integral can be computed using standard probability methods such as Monte Carlo sampling, First Order Reliability Method, importance sampling, and different methods can be used to compute the probability-of-failure and the fluxes.

The flux integral is evaluated by integrating the JPDF within the failure domain over the surface defined by $x_i = \theta_i$. However, the integration may proceed over the safe

domain defined by $P_{\bar{I}}^{\theta} = \int_{-\infty}^{\infty} \bar{I}(\mathbf{y},\theta) f_{\mathbf{Y}}(\mathbf{y}) d\mathbf{y}$, where $\bar{I}(\mathbf{y},\theta)$ equals one in the safe domain, zero otherwise (the complement to $I(\mathbf{y},\theta)$). Then the flux integral can be computed indirectly since $P_I^{\theta} + P_{\bar{I}}^{\theta} = 1$. Then $P_I^{\theta} = 1 - P_{\bar{I}}^{\theta}$.

Comparison between Eqs. (11) and (2) indicates that the numerical values of the probability-of-failure and the flux may be significantly different as the integrals are of different dimensions and domains. For example, consider upper right graphic in Figure 3 where the failure domain is a small sliver near the upper bound of X_1. As a result, the probability-of-failure, P_f, will be very small whereas the flux integral over the surface, P_I^b, will be equal to one since the integration of the joint PDF with respect to the remaining random variables integrates to one. Thus, P_f and P_I^b will have significantly different values.

The flux integrals are particularly straightforward to compute when using sampling as they are a subset of the probability integral. The sampling code for the probability-of-failure can be used with the only change of generating samples at the appropriate bound for the affected random variable. The necessary equations are

$$P_f \approx \frac{1}{m} \sum_{k=1}^{m} I(\mathbf{x}_k) \qquad \textbf{(12)}$$

$$P_I^{\theta} \approx \frac{1}{m} \sum_{k=1}^{m} I(\mathbf{y}_k, \theta) \qquad \textbf{(13)}$$

If sampling is used to compute P_f, it is possible to reuse the samples to compute P_I^a by projecting the samples onto the surface $X_i = a$ or $X_i = b$ thereby obtaining the sensitivities at negligible computational cost.

The flux integrals can also be computed using First/Second Order Reliability Method (FORM/SORM) by recasting the integrals in the N-1th dimension: the limit state is modified to $g(\mathbf{x} \mid x_i = \theta) = 0$, variable X_i is no longer random, and $f_{X_i} = f_{X_i}(\theta)$.

2.3 Maximum and Minimum Sensitivities

The probabilistic sensitivities, defined in Eqs. (9) and (10), are dependent upon the probability integrals P_f and P_I^a. Given that probability integrals are bounded by zero and one, it is straightforward to estimate the maximum and minimum magnitude the sensitivities may obtain. These estimates may be sufficient for preliminary design purposes.

The largest positive values of the sensitivities occur when $P_I^a = 0$, and $P_I^b = 1$, yielding

$$\begin{aligned} \left.\frac{\partial P_f}{\partial a_i}\right|_{Pos} &= f_{X_i}(a) P_f \\ \left.\frac{\partial P_f}{\partial b_i}\right|_{Pos} &= f_{X_i}(b)(1 - P_f) \end{aligned} \qquad \textbf{(14)}$$

Conversely, the minimum values of the sensitivities occur when $P_I^a = 1$, and $P_I^b = 0$, yielding

$$\begin{aligned} \left.\frac{\partial P_f}{\partial a_i}\right|_{Neg} &= -f_{X_i}(a)(1 - P_f) \\ \left.\frac{\partial P_f}{\partial b_i}\right|_{Neg} &= -f_{X_i}(b) P_f \end{aligned} \qquad \textbf{(15)}$$

In certain instances, it may be possible to have a priori knowledge of the failure domain along a bound of the truncated random variable, and, therefore, have an estimate

of the flux integral and the sensitivity. For example, if the random variable represents the load on a component, it may be known that the component will fail for a load equal to the upper bound of the random variable and not fail for a load equal to the lower bound of the random variable, regardless of the values of the other random variables. In such a case, the failure domain along the surfaces $x_i = a$ and $x_i = b$ is known a priori and in this case encompasses the entire surface defined by $x_i = b$ and none of the surface defined by $x_i = a$. Along the lower bound the flux integral is zero and along the upper bound the flux integral is one. In this case, the sensitivities are given in Eqs. (14) and no explicit evaluation of the flux integrals is required.

2.4 Properties of the Sensitivities

It is known that the sensitivities must satisfy certain properties [13, 18]. In particular, if the failure domain encompasses the entire random variable domain $I(\mathbf{x}) = 1$ everywhere, then the probability-of-failure is always one regardless of the values of the parameters; therefore, $\partial P_f / \partial \theta = 0$. This condition must be satisfied with respect to any parameter of the PDFs including bounds. When the failure domain encompasses the entire random variable domain $P_f = P_I^a = 1$ and the sensitivities are $\partial P_f / \partial \theta = 0$. From these results, we see that the kernel functions *must* have the forms $\kappa_a = f_X(a)$, $\kappa_a = -f_X(a)$ regardless of distribution type in order for $\partial P_f / \partial \theta = 0$ to be satisfied.

2.5 Variance estimates

Variance estimates for $\partial P_f / \partial \theta$ can be obtained by computing the variance of Eqs. (9) and (10). The formulation is straightforward as the variance of a linear function of random variables $\mathbf{X}$, e.g., $Y = \sum A_i X_i$, where $\mathbf{A}$ are constants, is known analytically as [20]

$$Var(Y) = \sum_{i=1} \sum_{j=1} A_i A_j \rho_{ij} \sigma_i \sigma_j \tag{16}$$

where σ_i represents the standard deviation of X_i, and ρ_{ij} denotes the correlation between X_i and X_j. Applying Eq. (16) to Eqs. (9) and (10), yields

$$V[\frac{\partial P_f}{\partial \theta}] = f_{X_i}^2(\theta)\left(V[P_f] + V[P_I^\theta] - 2\rho\sigma[P_f]\sigma[P_I^\theta]\right) \tag{17}$$

where ρ is the correlation between P_f and P_I^θ. It is clear from Eq. (17) that the correlation between P_f and P_I^θ affects the variance of the sensitivity estimate. Independent sampling can be chosen to ensure $\rho \approx 0$. A better approach is to employ "common" variables such that the correlation is greater than zero, i.e., $\rho > 0$, to minimize the variance [21, 20]. This is easily accomplished by using the same samples for the P_f and P_I^θ integrals. The reuse of samples by projecting the samples onto the bound of interest ensures positive correlation and provides an estimate of the flux integral without additional computational cost.

The variance estimates of P_f and P_I^θ are well known if Monte Carlo sampling is used to compute the probabilities, e.g., $V[P_f] \approx \frac{\overline{P}_f(1-\overline{P}_f)}{N}$ and $V[P_f] \approx \frac{\overline{P}_I^a(1-\overline{P}_I^a)}{N}$ where $\overline{P}_f$ and $\overline{P}_I^a$ are the sampling estimates of P_f and P_I^a.

3. Extension to Response Moments

In many mathematical and engineering problems, the sensitivity of the response moments (mean, μ_z, and standard deviation, σ_z) are of interest, where $Z(\mathbf{X})$ is an arbitrary output function of the random variables. The methodology derived in the previous sections can be extended to provide the probabilistic sensitivities of the response moments with respect to the bounds, e.g., $\partial\mu_Z/\partial a$ or $\partial\sigma_Z/\partial a$, see Appendix B.

3.1 Probabilistic sensitivity of the mean response with respect to bounds

The sensitivities of the response mean, μ_Z, to the bounds of a truncated PDF are, (see Appendix B)

$$\begin{aligned} \frac{\partial\mu_Z}{\partial a_i} &= f_{X_i}(a)(\mu_Z - P_Z^a) \\ \frac{\partial\mu_Z}{\partial b_i} &= -f_{X_i}(a)(\mu_Z - P_Z^b) \end{aligned} \qquad \textbf{(18)}$$

The flux calculation here is modified from Eq. (11) in that the indicator function is now replaced by the response function; therefore, the flux can be written as

$$\Gamma_Z^\theta = \int_{-\infty}^{\infty} Z(\mathbf{y},\theta)\, f_{\mathbf{X}}(\mathbf{y},\theta)d\mathbf{y} = f_{X_i}(\theta)P_Z^\theta \qquad \textbf{(19)}$$

where

$$P_Z^\theta = \int_{-\infty}^{\infty} Z(\mathbf{y},\theta)\, f_{\mathbf{Y}}(\mathbf{y},\theta) d\mathbf{y} \qquad \textbf{(20)}$$

The integration domain is again defined by the surface S defined by $x_i = \theta_i$. Although the probability integral P_I^θ must be positive, the flux integral P_Z^θ can be either positive or negative depending upon the response function Z.

3.2 Probabilistic sensitivity of the standard deviation of the response with respect to bounds

The sensitivities of the response standard deviation, σ_Z to the bounds of a truncated PDF are, (see Appendix B)

$$\frac{\partial \sigma_Z}{\partial a} = f_{X_i}(a)\{\sigma_Z^2 - \mu_Z^2 + 2\mu_Z P_Z^a - P_{Z^2}^a\}/(2\sigma_Z) \qquad \textbf{(21)}$$

$$\frac{\partial \sigma_Z}{\partial b} = -f_{X_i}(b)\{\sigma_Z^2 - \mu_Z^2 + 2\mu_Z P_Z^a - P_{Z^2}^\theta\}/(2\sigma_Z) \qquad \textbf{(22)}$$

where $P_{Z^2}^\theta = \int_{-\infty}^{\infty} Z^2(\mathbf{y},\theta)\, f_{\mathbf{Y}}(\mathbf{y}) d\mathbf{y}$. $P_{Z^2}^\theta$ must be always positive.

4. Numerical Examples

A two random variable problem amenable to exact integration both component and system, is solved in detail to demonstrate the methodology. This problem also provides a means to generate plots that clearly show the flux integrals.

4.1 Two random variable problem

A two dimensional example is solved to illustrate the concepts. Consider a limit state of $g(r,s) = r - s$ with *R* and *S* modeled as independent random variables. The indicator function defines the failure region as

$$I[r,s] = \begin{cases} 1 & \text{if } g(r,s) \le 0 \\ 0 & \text{otherwise} \end{cases} \quad \textbf{(23)}$$

R is a standard normal distribution and *S* is a uniform distribution with bounds $a = 0$ and $b = 1$.

$$f_R(r) = \frac{1}{\sqrt{2\pi}} Exp[-r^2/2] \qquad -\infty \le r \le \infty \quad \textbf{(24)}$$

$$f_S(s) = \begin{cases} 1 & 0 \le s \le 1 \\ 0 & \text{otherwise} \end{cases} \quad (25)$$

4.2 Probability-of-failure sensitivities

The JPDF over a portion of the failure domain ($-4 < r < 4$; $0 < s < 1$) is shown in Figure 4 with a direct view of the face $S = 1$. The exact solution from integration is $P_f = 0.68437$. The JPDF with a direct view of the face $S = 0$ is shown in Figure 5. The fluxes can be evaluated using one-dimensional integrals

$$P_I^a = f_S(a) \int_{-\infty}^{\infty} I(r,a)\, f_R(r) dr \quad \textbf{(26)}$$

$$P_I^b = f_S(b) \int_{-\infty}^{\infty} I(r,b)\, f_R(r) dr \quad \textbf{(27)}$$

Using symbolic integration, $P_I^a = 0.5$ and $P_I^b = 0.8413$. From Figures 4 and 5, it is clear that the integral of f_R over the failure surface where $S = 0$ equals $F_R(0) = \Phi(0)$ and the integral of f_R over the failure surface where $S = 1$ equals $F_R(1) = \Phi(1)$.

Table 1 summarizes results obtained using both the flux-based methodology and the standard finite difference (forward differencing) method. The derivatives of the probability-of-failure with respect to the bounds were computed using Eqs. (9) and (10). Finite difference estimates were computing using symbolic integration with a forward step size of 0.00001. The minimum and maximum sensitivities are $\partial P_f / \partial a = [-0.3157, 0.6843]$, and $\partial P_f / \partial b = [-0.6843, 0.3157]$.

Sampling estimates were computed using the equations $P_f \approx \frac{1}{N}\sum_{k=1}^{N} I(r_k, s_k)$, $P_I^a \approx \frac{1}{N}\sum_{k=1}^{N} I(r_k, a)$, and $P_I^b \approx \frac{1}{N}\sum_{k=1}^{N} I(r_k, b)$ with common random variables [21]. FORM analysis can also be used to compute the flux integrals. In this example, FORM reproduces the exact results.

The sensitivities for the flux-based and finite difference methods using exact integration are very close, as expected. The results using sampling are also in good agreement; however, note that 10^4 samples were used for the flux-based approach to obtain a solution with good accuracy versus 10^6 samples for the finite difference sampling-based approach. The superiority of the flux-based approach compared to the standard finite difference (forward differencing) approach using sampling can be shown clearly by comparing the 95% confidence bounds and the coefficient of variation (COV = standard deviation/mean) obtained using both methods obtained from 100 trials. Figures 6a and 6b show plots of the 95% confidence bounds for finite difference (dashed) versus

flux-based (solid) for $\partial P_f / \partial a$ and $\partial P_f / \partial b$, respectively. The bounds for the flux-based approach are so much narrower than the finite difference approach that they show almost as a straight line. The bounds are so wide for the finite difference method that any solution obtained is completely unreliable until the number of samples approaches one million.

A closer examination of the benefits of using common random variables during the sampling process is provided in Table 2. Variance results for negative, approximately zero, and positive sampling correlation are provided. The results clearly show that positive correlation provides approximately a three times reduction in the variance of the sensitivities with respect to independent sampling; at zero cost. Positive correlation was accomplished simply by using the same samples to compute the probability-of-failure and the fluxes. All subsequent results using sampling shown in the paper were computed using common variables, thereby inducing positive correlation.

Table 3 shows the coefficient of variation of the two methods as a function of the number of samples. The COV for the finite difference method is approximately two orders of magnitude larger than that obtained using the flux-based method for the same number of samples. These results imply that there are approximately 4 orders of magnitude difference in the number of samples required to achieve similar accuracy using both methods. The explanation is that the finite difference method requires an approximation of a limiting process estimated by subtracting two near-equal numbers. The flux-based approach, on the other hand, requires no limiting process nor subtraction of near-equal numbers. The results from Table 3 indicate that using the flux-based approach with 10^3 samples is superior to the finite difference method with 10^6 samples.

4.3 Response moments

Consider the previous PDFs with a response function $Z(r,s) = 5 + 5r - 2r - 5s - 4s^2$. Plots of Z times the JPDF are shown in Figures 7a and 7b and Z^2 times the JPDF are shown in Figures 8a and 8b. The profiles of the flux of $Z\ f_R$ and $Z^2 f_R$ along the boundaries $s = a$ and $s = b$ are clearly evident. Using numerical integration, the moments of Z are $\mu_Z = -0.8333$ and $\sigma_Z = 6.311$. The fluxes are $\Gamma_Z(\mathbf{y},a) = 3$, $\Gamma_Z(\mathbf{y},b) = -6$, $\Gamma_{Z^2}(\mathbf{y},a) = 42$, and $\Gamma_{Z^2}(\mathbf{y},b) = 69$. The sensitivities are given in Table 4. The flux-based and finite difference results using integration were very close, as expected.

The expected values of the sensitivities using sampling showed close agreement with the numerical integration results. However, similar to the sensitivities with respect to probability-of-failure shown in Tables 1 through 3, the COV of the sensitivities of the response moments using the finite difference approach was much larger than the flux-based method; 10% for $\partial\mu_Z/\partial a$ using finite difference with 10^6 samples versus 0.6% for the flux-based approach using 10^4 samples. The COV results for $\partial\sigma_Z/\partial a$ were 50% with for finite difference with 10^6 samples and 5% for the flux-based approach with 10^4 samples. Similar results were seen for $\partial\mu_Z/\partial b$ and $\partial\sigma_Z/\partial b$.

4.4. System reliability

The previous example was modified to demonstrate the applicability of the sensitivity methodology to system reliability problems. Two limit states were considered $g_1(r,s) = r - s$ and $g_2(r,s) = 5 - 5r + 2r^2 + 5s + 4s^2$. The system was analyzed as both a series and a parallel system.

4.4.1 Series system

For the series system, failure was defined as $P_f = P[g_1 \le 0 \bigcup g_2 \le 0]$. The JPDF in the failure region is shown in Figure 9. The JPDF along the bounds *a* and *b* needed for the flux calculations are shown in Figure 10a and Figure 10b, respectively. The results were $P_f = 0.70375$ (exact integration), $P_I^a = \Phi(0) + \Phi(-3.26557) = 0.5000546$, $P_I^b = 1$, $\partial P_f / \partial a = 0.203204$ and $\partial P_f / \partial b = 0.29625$. The sensitivities are shown in Table 5. The minimum and maximum sensitivities are $\partial P_f / \partial a = [-0.2962, 0.7038]$, and $\partial P_f / \partial b = [-0.7038, 0.2963]$. As shown in previous examples, the COV estimates using sampling for the finite difference method with 10^6 samples was approximately an order of magnitude larger than the COV for the flux-based method using 10^4 samples.

4.4.2 Parallel system

For the parallel system, failure was defined as $P_f = P[g_1 \le 0 \bigcap g_2 \le 0]$. The JPDF in the failure region is shown in Figure 11. The JPDF along the bound $S = 0$ is shown in Figure 12 and it is clear from the Figure 11 that the flux across the bound $S = 1$ is zero. The results from numerical integration were $P_f = 0.233742$, $P_I^a = \Phi(0) - \Phi(-0.76556) = 0.278031$, $P_I^b = 0$, $\partial P_f / \partial a = -0.0442901$ and $\partial P_f / \partial b = -0.233742$. The minimum and maximum sensitivities are $\partial P_f / \partial a = [-0.7663, 0.2337]$, and $\partial P_f / \partial b = [-0.2337, 0.7663]$. The sensitivities are shown in Table 6. Again, the COV for the flux-based method was significantly smaller than finite difference even with fewer samples.

5. Discussion and Conclusions

Efficient evaluation of the sensitivity of the probability-of-failure or the response moments to the bounds of truncated distributions can provide useful information in the design stage in order to optimize product reliability, minimize cost, determine quality assurance procedures, etc. The method outlined here can be used to compute these sensitivities with a significant improvement in computational efficiency over standard finite difference methods.

The methodology is based upon an application of the material derivative concept to the probability-of-failure or the response moment integrals thus yielding a flux integral that must be computed in addition to the standard probability-of-failure or response integrals. The methodology is applicable to any limit state formulation, either component or system, and any random variables described by a truncated joint probability density function containing either correlated, e.g., truncated multivariate normal, or independent random variables.

The sensitivities require a supplemental flux integral for each bound that, when combined with the probability-of-failure and kernel functions, provides the sensitivity with respect to the bound of a truncated distribution. However, the flux integral itself is a probability integral and, therefore, amenable to solution using existing probabilistic methods. Simple approximations to the flux integral are easily discerned which may avoid explicit calculation of the integral and provide an upper bound on the sensitivities. The magnitudes of the probability-of-failure and the flux integrals maybe significantly different and different methods may be used to compute each.

If sampling is used to compute the probability-of-failure, the samples can be reused to compute flux integrals by projecting the samples to the bound of interest. Thus, the flux integrals are computed with negligible additional computation.

The superiority of the flux-based approach over the standard finite difference method was clearly evident from numerical studies using Monte Carlo sampling that indicated that the estimate of the sensitivities using the flux-integral approach required approximately 4 orders of magnitude fewer samples for the same accuracy as a standard finite difference approach.

Acknowledgements

The research effort was supported in part by Contract FA8650-07-C-5060 (HM) from the Air Force Research Laboratory, RX Directorate, Pat Golden RXLMN project manager, and NIH grant K25CA116291 (YF).

Appendices

Appendix A - Kernel functions with respect to PDF bounds

The JPDF subjected to rectangular truncation, i.e., $x_i = \theta_i : \theta_i \in \mathbf{R}^n$ where θ_i corresponds to the lower (a) or upper (b) bound, can be written

$$f_{\mathbf{X}}(\mathbf{x}) = \begin{cases} \dfrac{\hat{f}_{\mathbf{X}}(\mathbf{x})}{\hat{F}_{X_i}(b) - \hat{F}_{X_i}(a)} & a \le x_i \le b \\ 0 & \text{otherwise} \end{cases} \qquad \textbf{(A-1)}$$

where $\hat{f}_{\mathbf{X}}(\mathbf{x})$ is the non-truncated JPDF, a and b are the lower and upper bounds of random variable X_i, and $\hat{F}_{X_i}$ denotes the CDF of X_i.

Consider the derivative with respect to the upper bound *b*

$$\frac{\partial \hat{f}_{\mathbf{X}}(\mathbf{x})}{\partial b} = \frac{\partial}{\partial b}\left(\frac{\hat{f}_{\mathbf{X}}(\mathbf{x})}{\hat{F}_{X_i}(b) - \hat{F}_{X_i}(a)}\right) =$$
$$\left(\frac{-\hat{f}_{\mathbf{X}}(\mathbf{x})}{\left(\hat{F}_{X_i}(b) - \hat{F}_{X_i}(a)\right)^2}\right)\frac{\partial \hat{F}_{X_i}(b)}{\partial b} =$$
$$\left(\frac{-\hat{f}_{\mathbf{X}}(\mathbf{x})}{\left(\hat{F}_{X_i}(b) - \hat{F}_{X_i}(a)\right)^2}\right)\hat{f}_{X_i}(b) = \qquad \textbf{(A-2)}$$
$$\frac{-\hat{f}_{\mathbf{X}}(\mathbf{x})}{\hat{F}_{X_i}(b) - \hat{F}_{X_i}(a)}\frac{\hat{f}_{X_i}}{\hat{F}_{X_i}(b) - \hat{F}_{X_i}(a)} =$$
$$-f_{\mathbf{X}}(\mathbf{x})\, f_{X_i}(b)$$

Therefore, the kernel function with respect to a rectangular bound $x_i = b$, where *b* is an upper bound, becomes

$$\kappa_b = \frac{\partial f_{\mathbf{X}}(\mathbf{x})}{\partial b}\frac{1}{f_{\mathbf{X}}(\mathbf{x})} = -f_{X_i}(b) \qquad \textbf{(A-3)}$$

Similarly

$$\kappa_a = \frac{\partial f_{\mathbf{X}}(\mathbf{x})}{\partial a}\frac{1}{f_{\mathbf{X}}(\mathbf{x})} = f_{X_i}(a) \qquad \textbf{(A-4)}$$

That is, the magnitude of the kernel function with respect to a bound of a random variable X_i is equal to the marginal distribution of X_i evaluated at the bound. The sign of the kernel function is dependent on the bound in consideration. These results are independent of distribution type.

Appendix B – Derivation of moment sensitivities

The sensitivity of the response mean μ_Z with respect to the distribution bounds is derived as an extension of the approach by Wu and Mohanty 2005 by adding the flux integral,

$$\frac{\partial \mu_Z}{\partial \theta_i} = \frac{\partial}{\partial \theta_i}\int_{-\infty}^{\infty} Z(\mathbf{x})\, f_{\mathbf{x}}(\mathbf{x})d\mathbf{x} \pm \Gamma_Z(\mathbf{y},\theta) = \int_{-\infty}^{\infty} Z(\mathbf{x})\kappa_\theta(\mathbf{x})\, f_{\mathbf{x}}(\mathbf{x})d\mathbf{x} \pm \Gamma_Z(\mathbf{y},\theta) = E[Z(\mathbf{x})\kappa_\theta(\mathbf{x})] \pm \Gamma_Z(\mathbf{y},\theta) \quad \textbf{(B-1)}$$

where $Z(\mathbf{x})$ represents the deterministic model response, $\kappa_\theta(\mathbf{x})$ represents the kernel functions. Using the kernel functions defined in Eqs. (6) and (7),

$$\frac{\partial \mu_Z}{\partial a} = f_{X_i}(a)\mu_Z - \Gamma_Z(\mathbf{y},a)$$
$$\frac{\partial \mu_Z}{\partial b} = -f_{X_i}(b)\mu_Z + \Gamma_Z(\mathbf{y},b) \quad \textbf{(B-2)}$$

Since $\Gamma_Z(y,\theta) = f_X(\theta)P_Z^\theta$, the sensitivities become

$$\frac{\partial \mu_Z}{\partial a} = f_{X_i}(a)(\mu_Z - P_Z^a)$$
$$\frac{\partial \mu_Z}{\partial b} = -f_{X_i}(a)(\mu_Z - P_Z^b) \quad \textbf{(B-3)}$$

The sensitivities of the standard deviation of the response with respect to the bounds of a random variable PDF can be determined by extending the derivation of Sues and Cesare [17] through the addition of the flux integrals to yield

$$\frac{\partial \sigma_Z}{\partial a} = (E[Z^2\kappa_a] - \Gamma_{Z^2}(\mathbf{y},a) - 2\mu_Z(E[Z\kappa_a] - \Gamma_Z(\mathbf{y},a)))/(2\sigma_Z) =$$
$$(f_{X_i}(a)E[Z^2] - \Gamma_{Z^2}(\mathbf{y},a) - 2\mu_Z(f_{X_i}(a)E[Z] - \Gamma_Z(\mathbf{y},a)))/(2\sigma_Z) =$$
$$(f_{X_i}(a)(\sigma_Z^2 + \mu_Z^2) - f_{X_i}(a)P_{Z^2}^a - 2\mu_Z(f_{X_i}(a)\mu_Z - f_{X_i}(a)P_Z^a))/(2\sigma_Z) =$$
$$f_{X_i}(a)\left\{\sigma_Z^2 - \mu_Z^2 + 2\mu_Z P_Z^a - P_{Z^2}^a\right\}/(2\sigma_Z) \qquad \textbf{(B-4)}$$

Where we have used the fact that $E[Z^2] = \sigma_Z^2 + \mu_Z^2$, $\Gamma_Z(\mathbf{y},\theta) = f_X(\theta)P_Z^\theta$, and $\Gamma_{Z^2}(\mathbf{y},\theta) = f_X(\theta)P_{Z^2}^\theta$.

A similar derivation for $\partial\sigma_Z/\partial b$ yields

$$\frac{\partial \sigma_Z}{\partial b} = (E[Z^2\kappa_b] + \Gamma_{Z^2}(\mathbf{y},b) - 2\mu_Z(E[Z\kappa_b] + \Gamma_Z(\mathbf{y},b)))/(2\sigma_Z) =$$
$$(-f_{X_i}(b)E[Z^2] + f_{X_i}(b)P_{Z^2}^b - 2\mu_Z(-f_{X_i}(b)E[Z] + f_{X_i}(b)P_Z^b))/(2\sigma_Z) =$$
$$(-f_{X_i}(b)(\sigma_Z^2 + \mu_Z^2) + f_{X_i}(b)P_{Z^2}^b - 2\mu_Z(-f_{X_i}(b)\mu_Z + f_{X_i}(b)P_Z^b))/(2\sigma_Z) =$$
$$-f_{X_i}(b)\left\{\sigma_Z^2 - \mu_Z^2 + 2\mu_Z P_Z^b - P_{Z^2}^b)\right\}/(2\sigma_Z) \qquad \textbf{(B-5)}$$

References

1. Grandt, AF Jr., *Fundamentals of Structural Integrity*, J. Wiley & Sons, Inc., 2004, Hoboken, NJ
2. Broek, D, 1989, *The Practical Use of Fracture Mechanics*, Springer
3. Subteam to the Aerospace Industries Association Rotor Integrity Subcommittee, 1997, ‘‘The Development of Anomaly Distributions for Aircraft Engine Titanium Disk Alloys,’’ 38th AIAA/ASME/ASCE/AHS/ASC SDM Conference, pp. 2543–2553.
4. Frey, HC and Patil SR, 2002, “Identification and Review of Sensitivity Analysis Methods,” Risk Analysis, Vol. 22, No. 3, pp. 553-578

5. Helton J, Johnson JD, Sallaberry CJ, and Storlie CB, 2006, “Survey of Sampling-Based Methods for Uncertainty and Sensitivity Analysis,” Reliability Engineering and System Safety 91, pp. 1175–1209
6. Sobol’ IM, 2001, “Global Sensitivity Indices for Nonlinear Mathematical Models and Their Monte Carlo Estimates,” Mathematics and Computers in Simulation; 55 (1-3): 271-280
7. Homma T, Saltelli A, 1996, “Importance Measures in Global Sensitivity Analysis of Nonlinear Models,” Reliability Engineering and System Safety,” 52: 1-17
8. Cukier RI, Fortuin CM, Schuler KE, Petschek AG, Schaibly JH, 1973, “Study of the Sensitivity of Coupled Reaction Systems to Uncertainties in Rate Coefficients I. Theory.” J Chem Phys;59(8):3873-8
9. Liu, H, Chen W, Sudjianto A, 2006, “Relative Entropy Based Method for Probabilistic Sensitivity Analysis in Engineering Design,” ASME Journal of Mechanical Design; 128: pp.326-336.
10. Madsen HO, Krenk L, Lind NC, 2006, *Methods of Structural Safety*, Dover Publications.
11. Madsen HO, 1988, “Omission sensitivity factors,” Structural Safety, 5(1): 35-45.
12. Kleijnen JRC and Rubinstein RY, 1996,. “Optimization and Sensitivity Analysis of Computer Simulation Models by the Score Function Method.” *European Journal of Operational Research* 88, 413-427
13. Rubinstein RY and Shapiro A, 1993, *Discrete Event Systems, Sensitivity Analysis and Stochastic Optimization by the Score Function Method*. J. Wiley & Sons, Chichester, England

14. Karamchandani AK, 1990, “New Approaches to Structural System Reliability,” Ph.D. thesis, Dept. of Civil Engineering, Stanford University 1990
15. Wu Y-T, 1994, “Computational Methods for Efficient Structural Reliability and Reliability Sensitivity Analysis.” *AIAA Journal* 32(8), 1717-1723
16. Wu Y-T and Mohanty S, 2006, “Variable Screening and Ranking Using Sampling-Based Sensitivity Measures,” Reliability Engineering and System Safety, 91: 634–647
17. Sues RH and Cesare MA, 2005, “System Reliability and Sensitivity Factors via The MPPSS Method,” Probabilistic Engineering Mechanics 20(2), 148–157
18. Millwater HR, 2009, “Universal Properties of Kernel Functions for Probabilistic Sensitivity Analysis,” Probabilistic Engineering Mechanics (accepted), doi:10.1016/j.probengmech.2009.01.005
19. Fung YC, 1965, *Foundations of Solid Mechanics*, Prentice-Hall, pp. 120-121
20. Ang AH-S and Tang, WH, 1984, *Probability Concepts in Engineering Planning and Design, Volume II*, J. Wiley & Sons, Inc.
21. Rubinstein RY and Kroese DP, 2007, *Simulation and the Monte Carlo Method*, 2nd Ed., Wiley-Interscience

Tables

	Flux-based		Finite Difference	
	Integration (exact)	Sampling (10^4 samples)	Integration (exact)	Sampling (10^6 samples)
$\frac{\partial P_f}{\partial a}$	0.1844	0.1842[1]	0.1844	.1876[1]
$\frac{\partial P_f}{\partial b}$	0.1560	0.1571[1]	0.1570	.1608[1]

[1]expected value of 100 trials)

Table 1 Probabilistic sensitivity results for limit state $g = r - s$ **(R standard normal, S uniform)**

# Samples	$\frac{\partial P_f}{\partial a}$ ($\rho < 0$)	$\frac{\partial P_f}{\partial a}$ ($\rho \approx 0$)	$\frac{\partial P_f}{\partial a}$ ($\rho > 0$)	$\frac{\partial P_f}{\partial b}$ ($\rho < 0$)	$\frac{\partial P_f}{\partial b}$ ($\rho \approx 0$)	$\frac{\partial P_f}{\partial b}$ ($\rho > 0$)
10^3	8.81E-4 (ρ=-0.75)	4.64E-4 (ρ~0)	1.37E-4 (ρ=0.82)	4.84E-4 (ρ=-0.46)	3.48E-4 (ρ~0)	1.29E-4 (ρ=0.78)
10^4	7.37E-4 (ρ=-0.66)	4.01E-5 (ρ=0.09)	1.44E-5 (ρ=0.68)	4.03E-4 (ρ=-0.27)	2.70E-5 (ρ=0.09)	1.22E-5 (ρ=0.64)

Table 2 Variance of sensitivity estimates $\partial P_f / \partial \theta$ as a function of sampling correlation (100 trials) – actual correlation in parentheses

	Flux-based		Finite Difference	
# Samples	$\frac{\partial P_f}{\partial a}$	$\frac{\partial P_f}{\partial b}$	$\frac{\partial P_f}{\partial a}$	$\frac{\partial P_f}{\partial b}$
10^3	.076	.063	4.4	8.9
10^4	.019	.022	2.1	1.8
10^5	.0076	.0076	.61	0.66
10^6	.0021	.0025	.16	0.22

Table 3 Coefficient of variation (100 trials) of sensitivities with respect to bounds as a function of the number of samples

	Flux-based		Finite Difference	
	Integration (numerical)	Sampling (10^4 samples)	Integration (numerical)	Sampling (10^6 samples)
$\frac{\partial \mu_Z}{\partial a}$	-3.833	-3.839[1] (0.6%)	-3.833	-3.848[1] (10%)
$\frac{\partial \mu_Z}{\partial b}$	-5.167	-5.161[1] (0.5%)	-5.167	-5.153[1] (8%)
$\frac{\partial \sigma_Z}{\partial a}$	-0.6223	-0.6280[1] (5%)	-0.6223	-0.6691[1] (50%)
$\frac{\partial \sigma_Z}{\partial b}$	1.573	1.569[1] (2.5%)	1.573	1.551[1] (22%)

[1]expected value of 100 trials

Table 4 Sensitivity results for response moments; COV results in parentheses based on 100 trials

	Flux-based		Finite Difference	
	Integration (exact)	Sampling (10^4 samples)	Integration (exact)	Sampling (10^6 samples)
$\frac{\partial P_f}{\partial a}$	0.2032	0.2031[1] (1.6%)	0.2032	0.2116[1] (18%)
$\frac{\partial P_f}{\partial b}$	0.2963	0.2963[1] (1.3%)	0.2965	0.3016[1] (13%)

[1]expected value of 100 trials

Table 5 Sensitivity results for series system; COV results in parentheses based on 100 trials

	Flux-based		Finite Difference	
	Integration (exact)	Sampling (10^4 samples)	Integration (exact)	Sampling (10^6 samples)
$\frac{\partial P_f}{\partial a}$	-0.04429	-.04396[1] (12%)	-0.04429	-0.04821[1] (111%)
$\frac{\partial P_f}{\partial b}$	-0.2337	-0.2331[1] (2%)	-0.2337	-0.2207[1] (22%)

[1]expected value of 100 trials

Table 6 Sensitivity results for parallel system; COV results in parentheses based on 100 trials

List of Figures

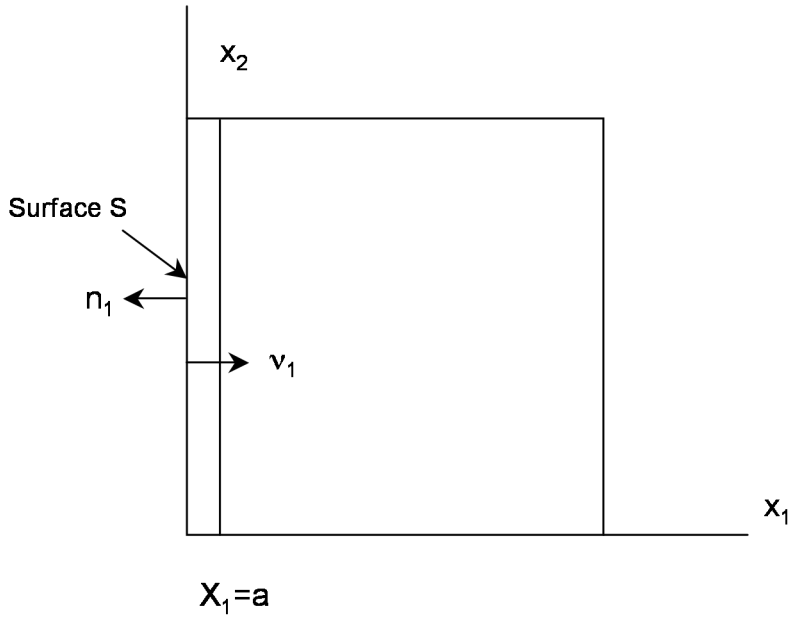

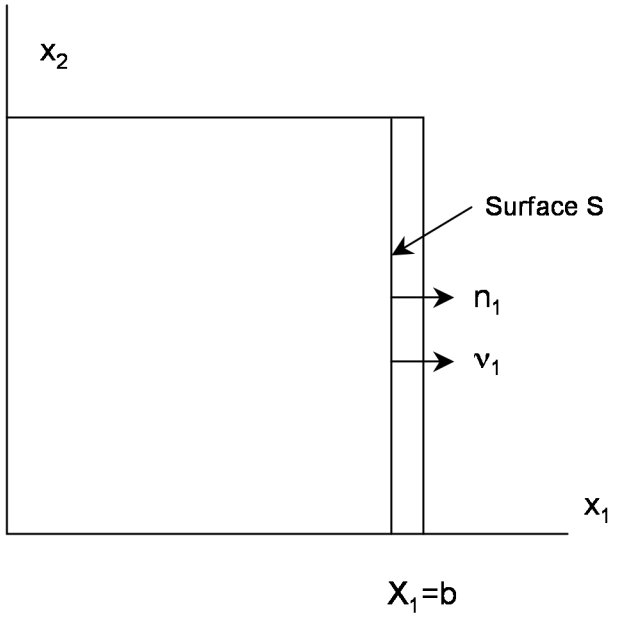

Figure 1 Description of velocity and unit normal along bounds

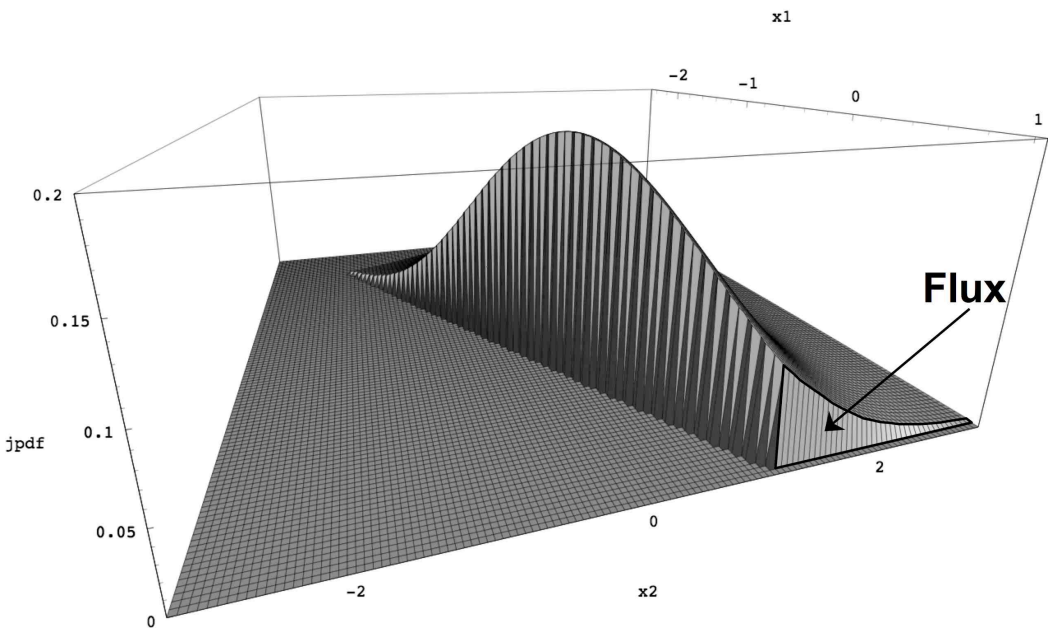

Figure 2 Flux of the JPDF in the failure region over the surface S

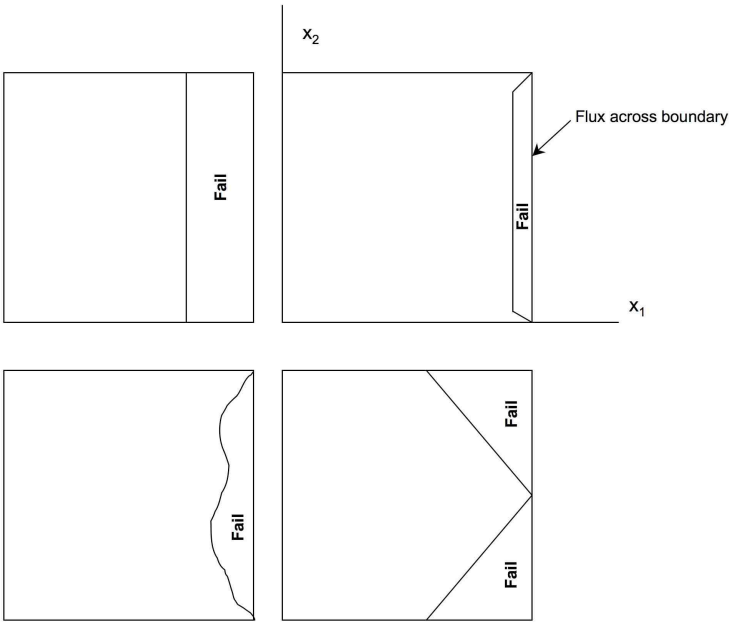

Figure 3 Two dimensional problems with the same flux values with respect to lower and upper bounds

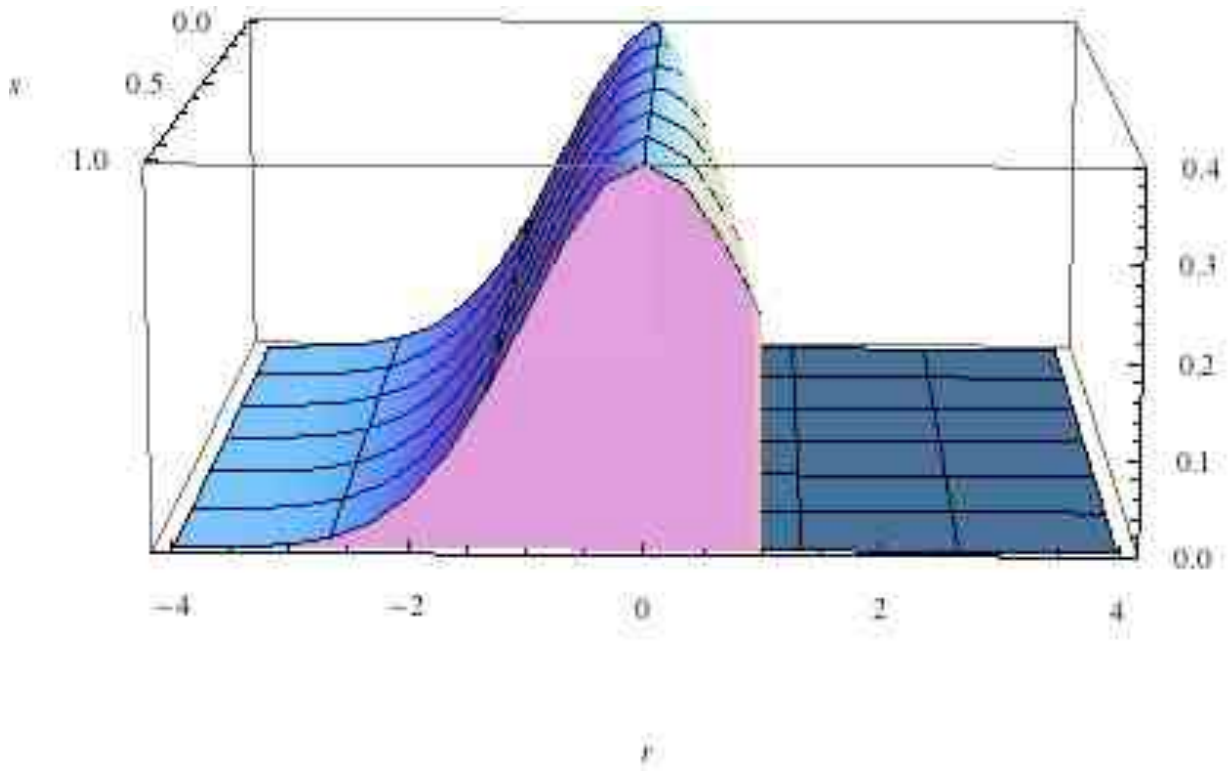

Figure 4 Joint PDF over failure domain (direct view of the face of $S = 1$)

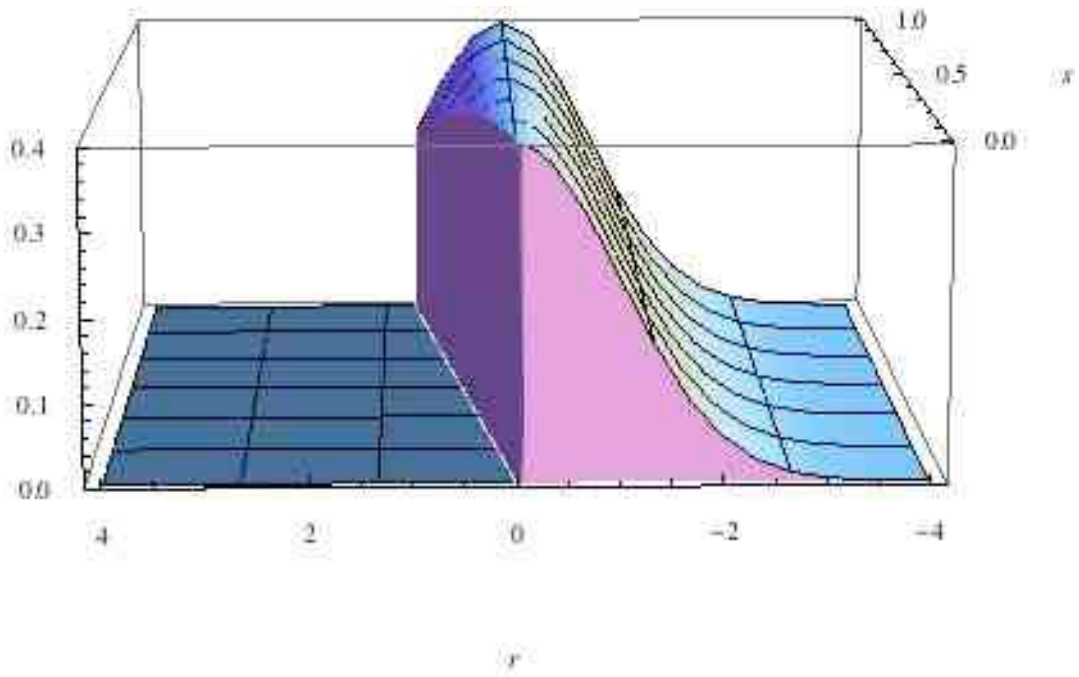

Figure 5 Joint PDF over failure domain (direct view of the face of $S = 0$)

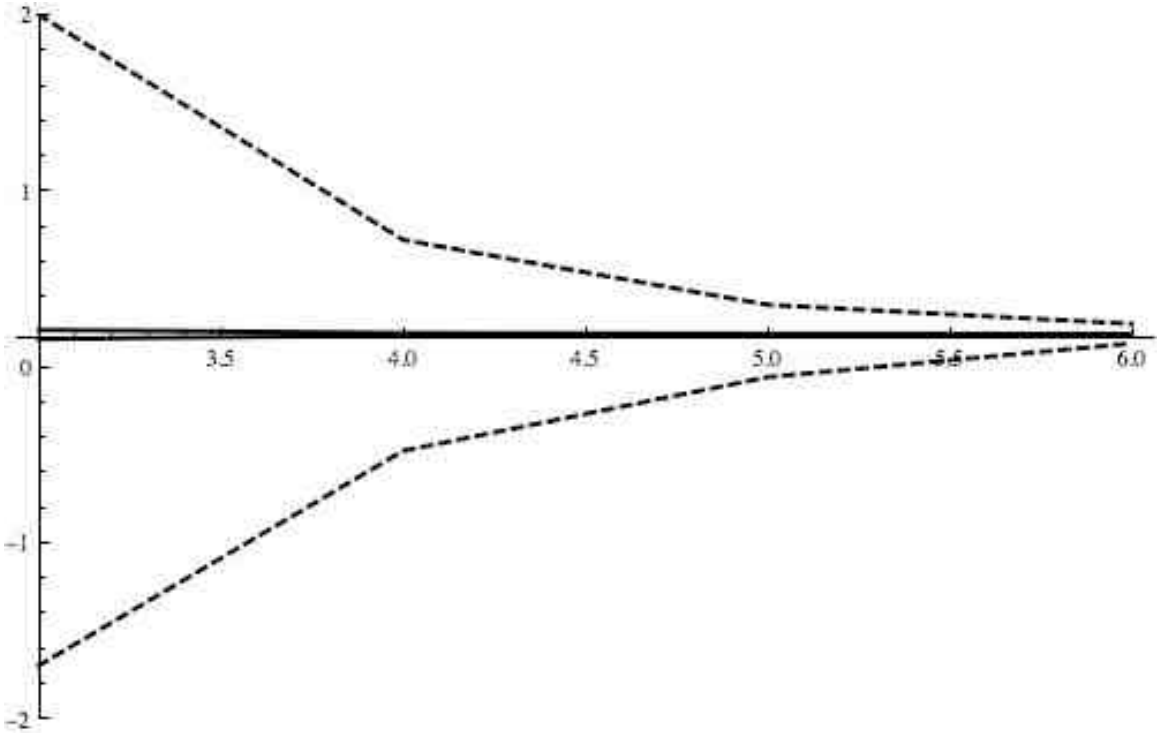

Figure 6a 95% confidence limits (100 trials) for $\partial P_f / \partial a$ as a function of the number of samples (dashed - finite difference; solid – flux based)

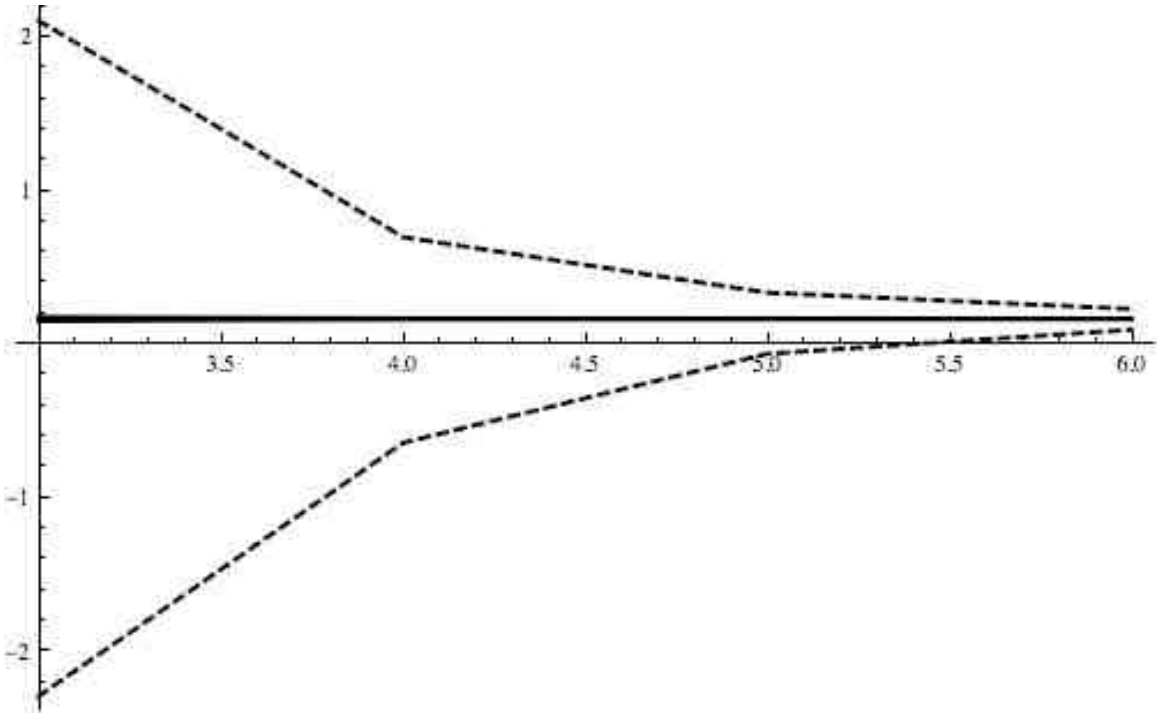

Figure 6b 95% confidence limits (100 trials) for $\partial P_f / \partial b$ as a function of the number of samples (dashed - finite difference; solid – flux based)

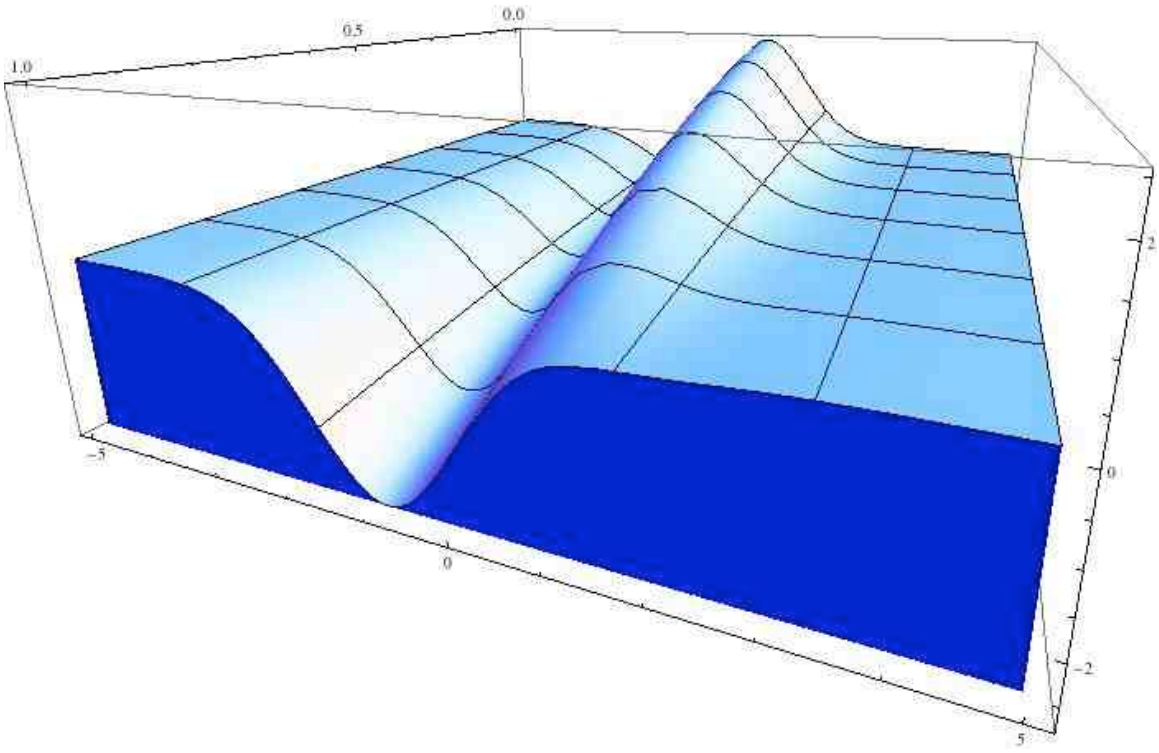

Figure 7a Plot of JPDF times Z (direct view of the face $S = 1$)

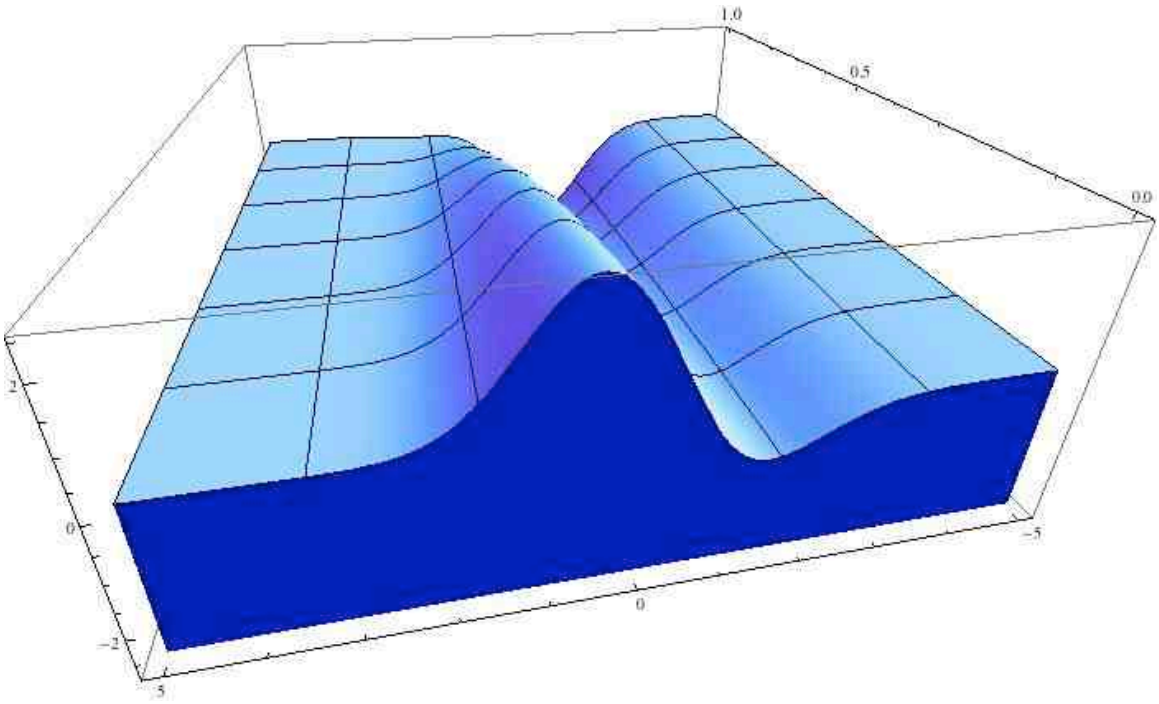

Figure 7b Plot of JPDF times Z (direct view of the face $S = 0$)

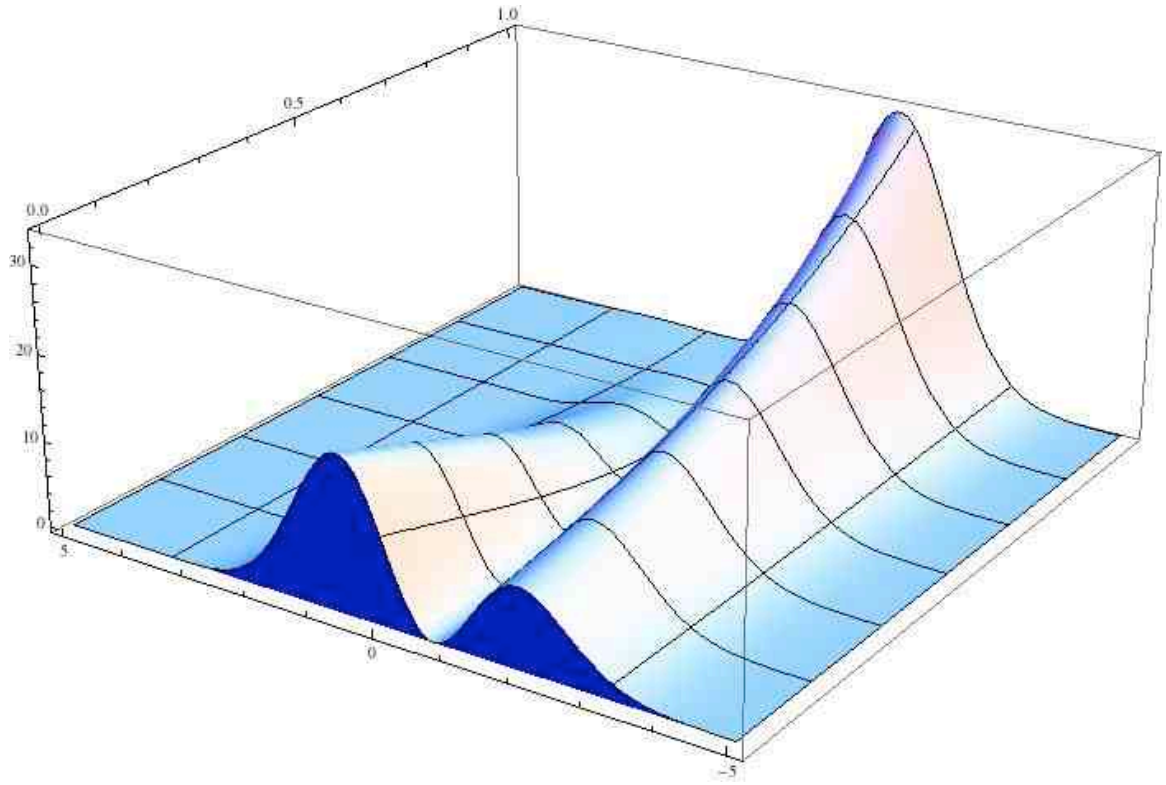

Figure 8a Plot of JPDF times Z^2 (direct view of the face $S = 0$)

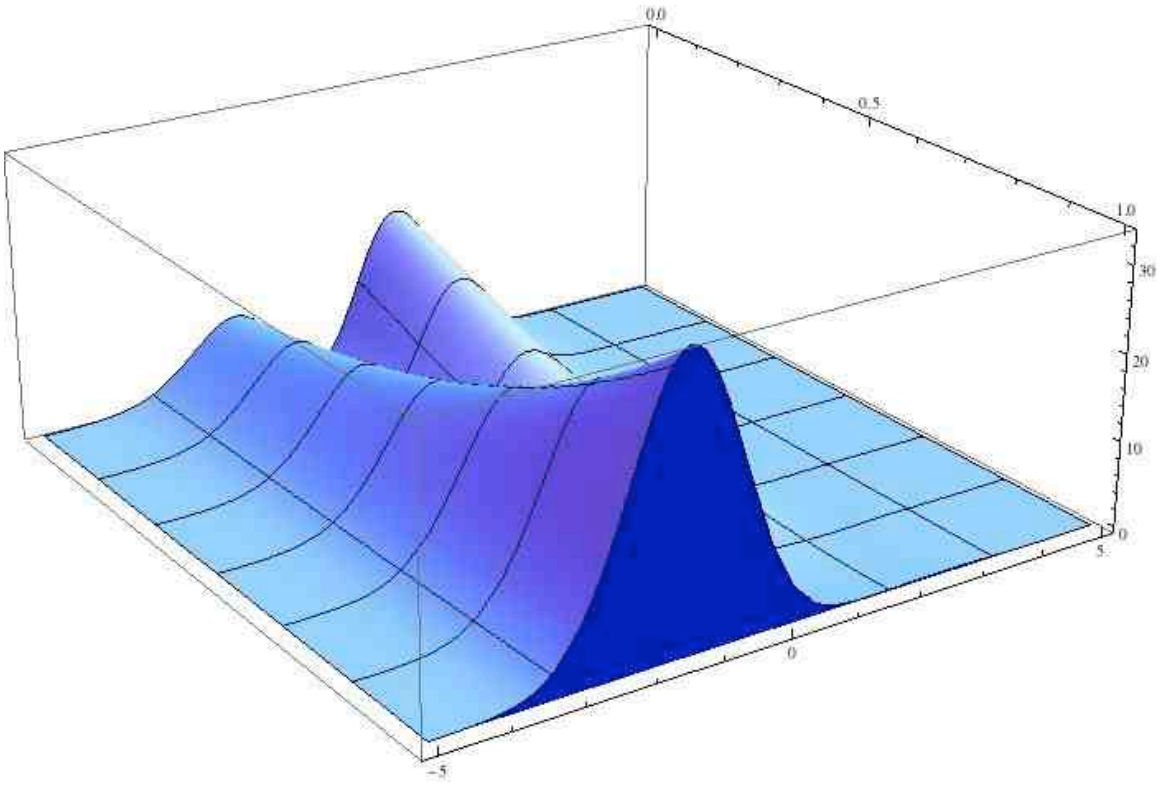

Figure 8b Plot of JPDF times Z^2 (direct view of the face $S = 1$)

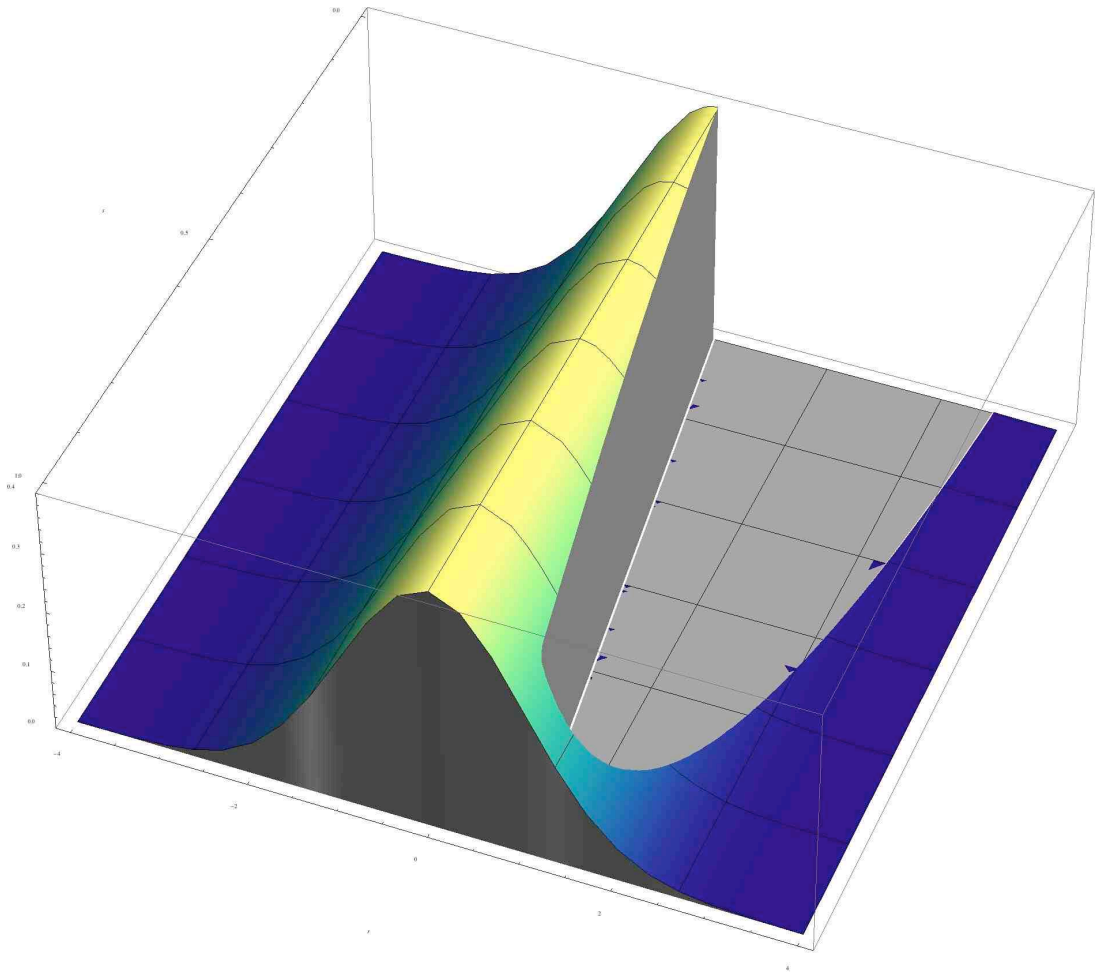

Figure 9 JPDF of series system

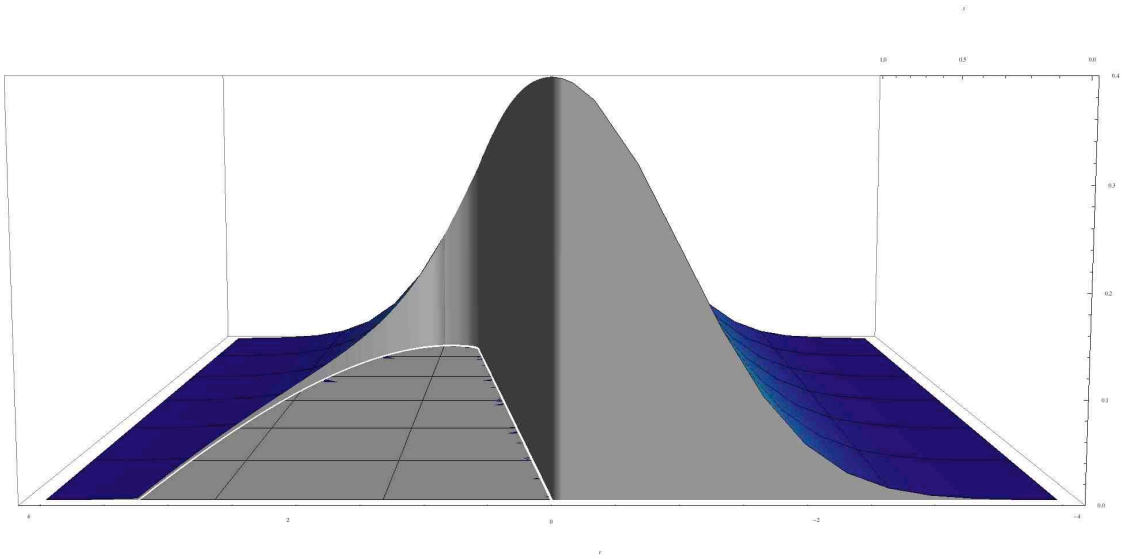

Figure 10a Flux along bound $S = 0$ for series system

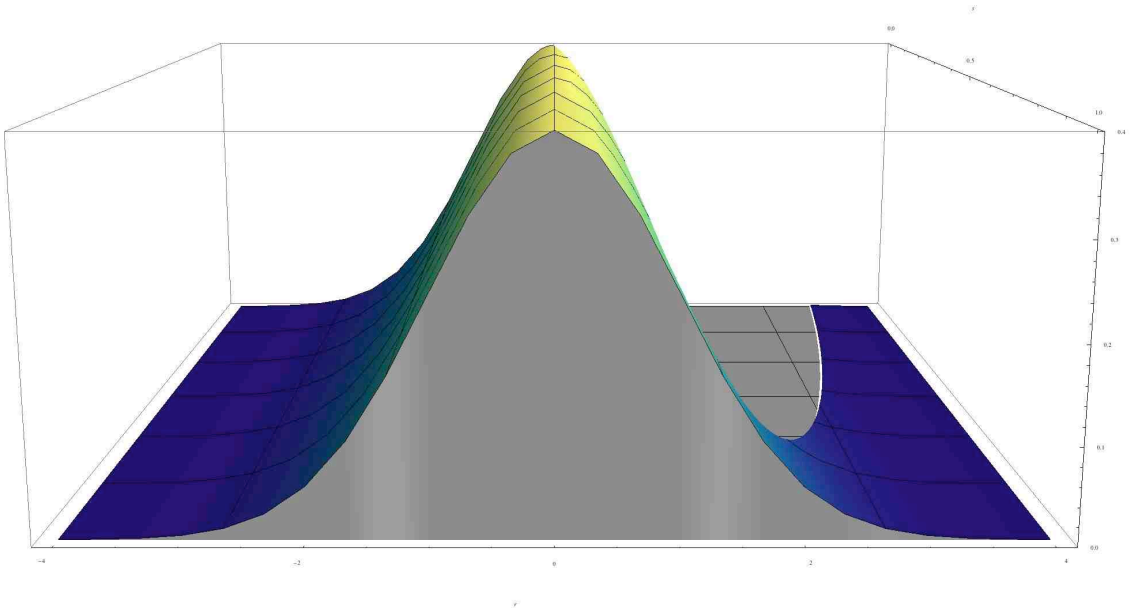

Figure 10b Flux along bound $S = 1$ for series system

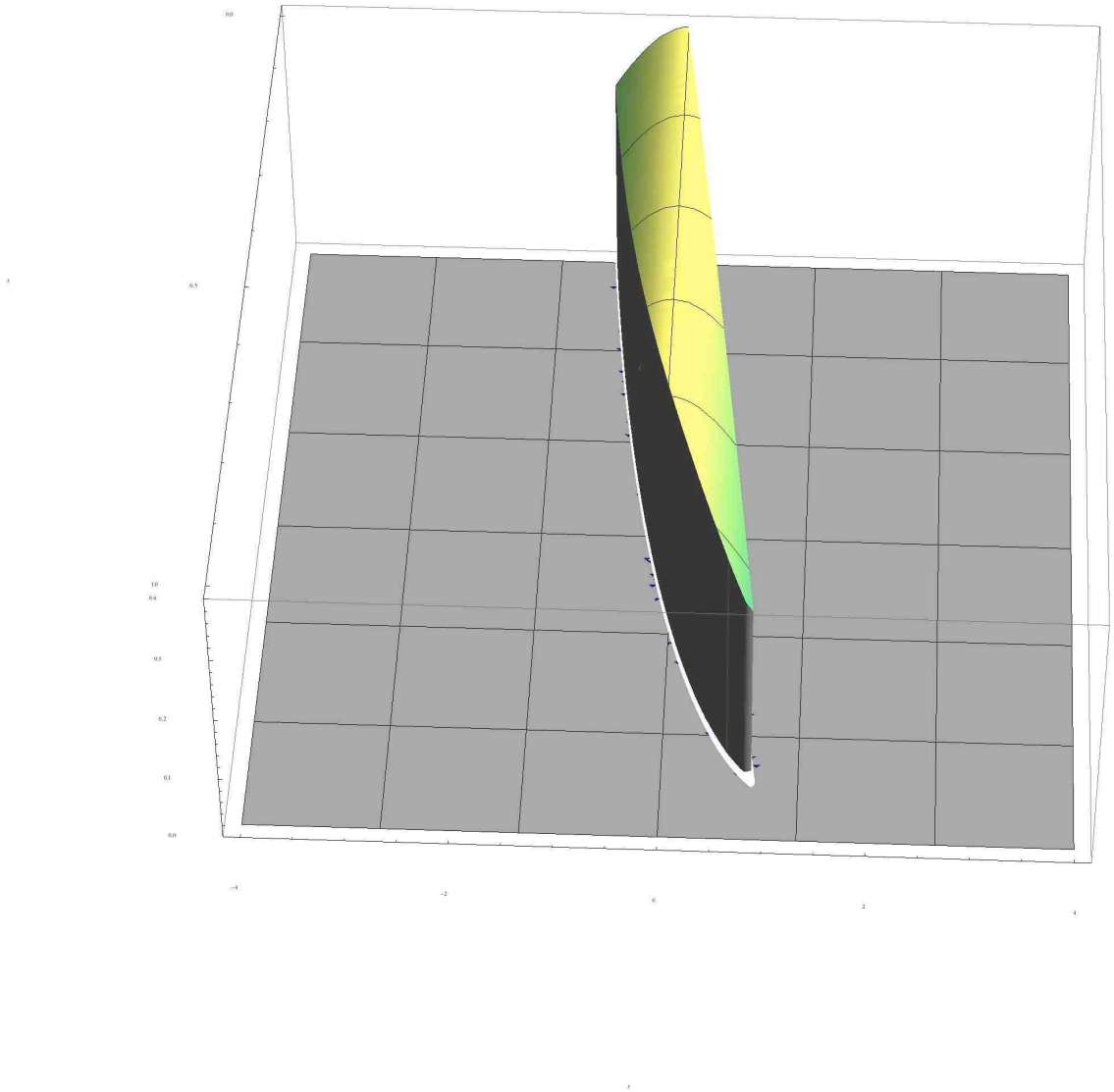

Figure 11 JPDF of parallel system

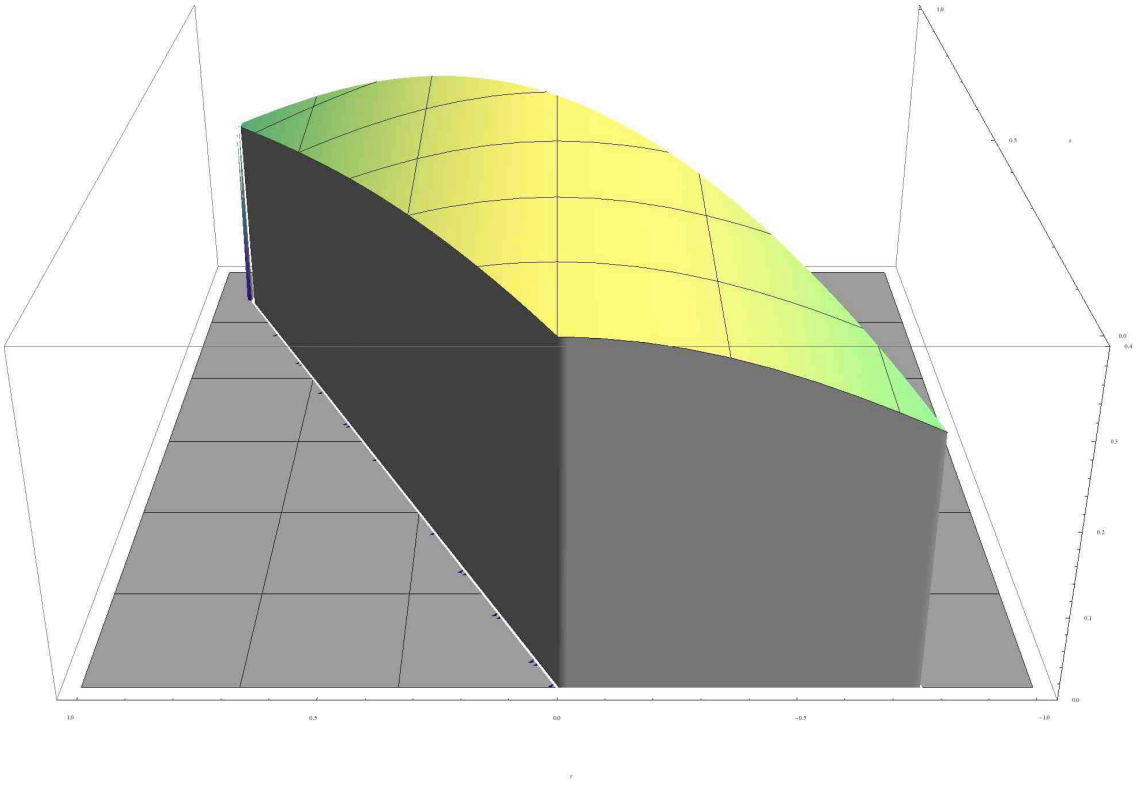

Figure 12 Flux along bound *a* of JPDF along bound a for parallel system